

Fundamental equations for primary fluid recovery from porous media

Yan Jin¹ and Kang Ping Chen^{2,†}

¹State Key Laboratory of Petroleum Resources and Prospecting, China University of Petroleum–Beijing, Beijing 102249, China

²School for Engineering of Matter, Transport and Energy, Arizona State University, Tempe, AZ 85287-6106, USA

(Received 3 May 2018; revised 23 October 2018; accepted 23 October 2018;
first published online 4 December 2018)

Primary fluid recovery from a porous medium is driven by the volumetric expansion of the *in situ* fluid. For production from a petroleum reservoir, primary recovery accounts for more than half of the total amount of recovered hydrocarbon. The primary recovery process is studied here at the pore scale and the macroscopic scale. The pore-scale flow is first analysed using the compressible Navier–Stokes equations and the mathematical theory for low-Mach-number flow developed by Klainerman & Majda (*Commun. Pure Appl. Maths*, vol. 34 (4), 1981, pp. 481–524; vol. 35 (5), 1982, pp. 629–651). An asymptotic analysis shows that the pore-scale flow is governed by the self-diffusion of the fluid and it exhibits a slip-like mass flow rate, even though the velocity satisfies the no-slip condition on the pore wall. The pore-scale density equation is then upscaled to a macroscopic diffusion equation for the density which possesses a diffusion coefficient proportional to the fluid’s kinematic viscosity. Darcy’s law is shown to be inapplicable to primary fluid recovery and it should be replaced by a new mass flux equation which depends on the porosity but not on the permeability. This is in stark contrast to the classical result and it can have important implications for hydrocarbon recovery as well as other applications.

Key words: low-Reynolds-number flows, Navier–Stokes equations, porous media

1. Introduction

Extracting a fluid stored in a porous medium is a problem of fundamental interest to many applications, such as hydrocarbon recovery, geothermal energy harvesting, filtration and bioengineering. When the porous medium is rigid and no fresh fluid is injected into the fluid-bearing reservoir to drive the *in situ* fluid out of the pore space, fluid recovery relies entirely on the volumetric expansion of the fluid; such a process is called primary recovery in the petroleum literature (Muskat 1949). Primary recovery is the first and the most important stage of hydrocarbon recovery, as it often accounts for more than half of the total amount of hydrocarbon recovered from a petroleum reservoir (Dake 1978). Like all flows through porous media, primary fluid

† Email address for correspondence: k.p.chen@asu.edu

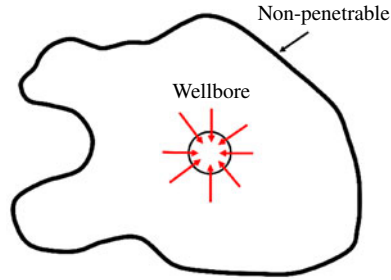


FIGURE 1. (Colour online) Schematic of primary fluid recovery from a porous reservoir. The outer boundary is impenetrable and the fluid is produced from the inner boundary (e.g. wellbore).

recovery has been studied using Darcy's law (Darcy 1856) for more than 80 years (Muskat 1937, 1949; Bear 1972; Scheidegger 1974; Dake 1978). As reviewed by Lasseux & Valdes Parada (2017), theoretical justification of Darcy's law did not appear until more than 100 years after Darcy's experiment, when it was shown that the macroscopic-scale Darcy's law can be derived from the pore-scale Stokes flow equation by the method of volume averaging or homogenization (Whitaker 1966, 1986; Keller 1980; Auriault 1987). This direct connection to the fundamental equations of fluid dynamics provides a solid theoretical support for broad application of Darcy's law to flows in porous media. While many of these derivations were based on the steady incompressible Stokes equation at the pore scale, notably Keller (1980) and more recently Masmoudi (2002) employed general compressible Navier–Stokes equations in their derivations. The leading-order problem from which Darcy's law is derived, however, is still an incompressible flow problem.

Primary fluid recovery from a porous medium is an inherently unsteady process occurring in a reservoir with a sealed outer boundary (figure 1). For a hydrocarbon reservoir, the outer boundary can be considered as impenetrable by fluids from the outside on the production time scale, which is of the order of several months to several years (but not on a geological time scale). Since no fresh fluid is injected into the reservoir, primary fluid recovery is driven by the volumetric expansion of the *in situ* fluid. Expansion of the porous rock occurs over a much larger time scale, since the rock's bulk modulus is several orders of magnitude higher than that of the fluid; and rock expansion also requires a significant drawdown in the pore pressure, which can only occur in the very late stage of primary recovery when significant fluid depletion has already taken place. Thus, despite a very low fluid velocity, which would normally justify the incompressible flow approximation from the classical gas dynamics arguments based on a vanishing Mach number, the flow during primary fluid recovery is physically dominated by the fluid's compressible effect. Recently, Chen & Shen (2018a,b) have studied fluid-expansion-driven drainage flow of a viscous compressible fluid from a semi-sealed small cylindrical capillary, which can be considered as a simple pore-scale model for primary recovery (figure 2). They solved the linearized compressible Navier–Stokes equations subject to the no-slip condition. Their results show that the fluid mass production rate from the capillary is proportional to the fluid's kinematic viscosity; and the no-slip drainage flow exhibits a slip-like mass flow rate proportional to the square of the capillary radius. These pore-scale results differ fundamentally from those for a Poiseuille-type flow, which

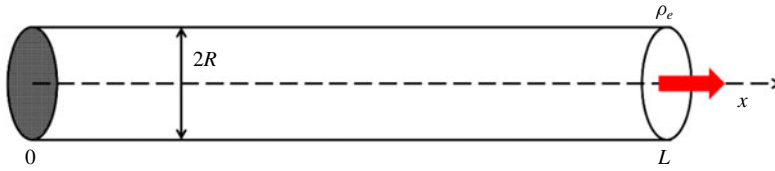


FIGURE 2. (Colour online) Primary recovery: a simple pore-scale model of draining a compressed fluid from a semi-sealed small capillary (from Chen & Shen 2018a). The exit density ρ_e is lower than the initial density ρ_i .

produces a mass flow rate inversely proportional to the fluid's kinematic viscosity and proportional to the quartic of the pore radius. Thus, it is expected that, when these pore-scale results are upscaled, the corresponding macroscopic mass flow rate will not obey Darcy's law, which is the upscaled version of the pore-scale Poiseuille's law. This indicates that, at the macroscopic scale, primary fluid recovery is not governed by Darcy's law.

The present study on primary fluid recovery starts from the pore-scale compressible Navier–Stokes equations with no-slip condition and derives the corresponding macroscopic-scale governing equations. It assumes that the condition for slip at the pore scale (Lasseux *et al.* 2014; Lasseux, Valdes Parada & Porter 2016) is not met and the no-slip condition applies. For simplicity and clarity, the present work is limited to a single-phase fluid; and the motion of a compressible fluid in the pore space is treated as a viscous compressible flow. Such a compressible flow is characterized by a small global Mach number, which is defined as the ratio between a reference fluid speed v_{ref} and a reference speed of sound c_{ref} , $M = v_{ref}/c_{ref} \ll 1$. An appropriate choice of the reference speed is the diffusion speed based on the longitudinal mass diffusion, D/L_{ref} , with D being the mass diffusion coefficient and L_{ref} the length of the medium. The flow is close to the incompressible limit of compressible flows, yet the compressible effect dominates the dynamics, as the flow in primary fluid recovery is solely driven by the volumetric expansion of the fluid. While it is widely known that the vanishing-Mach-number limit of the compressible Navier–Stokes equations converges to the incompressible Navier–Stokes equations, this limiting process is actually subtle, since the speed of sound tends to infinity and the governing equations change their type (Klainerman & Majda 1981). This low-Mach-number limit has attracted significant attention since the pioneering work of Ebin (1977, 1982) and Klainerman & Majda (1981, 1982) (see e.g. Schochet 1987a,b, 2005; Klein 1995; Lions & Masmoudi 1998; Desjardins & Grenier 1999; Desjardins & Lin 1999; Desjardins *et al.* 1999; Masmoudi 2000, 2007; Danchin 2001, 2002, 2005; Alazard 2006; Feireisl & Novotny 2009). We will first employ asymptotic expansions based on the work of Klainerman & Majda (1982) and the Helmholtz decomposition theorem to derive asymptotic equations for low-Mach-number viscous compressible flow at the pore scale for primary recovery. It will be shown that, for primary fluid recovery, the limiting incompressible field at a vanishing Mach number is identically zero and density is the primary variable of concern. The leading-order equations show that density change is controlled by the longitudinal mode of the acoustic field; while the role of the transverse mode (or solenoidal field) is to enforce the no-slip boundary condition on the pore wall. Density change obeys a damped wave equation; and at large times, this damped wave equation reduces to a diffusion equation with mass transport driven by the self-diffusion of the compressible fluid.

The pore-scale density diffusion equation is then upscaled using the method of volume averaging (Whitaker 1999) to obtain a macroscopic-level density diffusion equation. The new macroscopic-scale diffusion equation is compared to the classical macroscopic-scale equation based on Darcy’s law. It will be shown that there is a fundamental difference in the diffusion coefficients between the present and the classical results. The new macroscopic-level diffusion equation for the averaged density possesses a diffusion coefficient that is independent of the permeability but proportional to the fluid’s kinematic viscosity, instead of proportional to the permeability and inversely proportional to the kinematic viscosity for the classical diffusion coefficient based on Darcy’s law. The new diffusion coefficient can be several orders of magnitude larger than the classical diffusion coefficient. The analysis will show that Darcy’s law is not applicable to, and permeability plays no role in determining the production rate for, primary fluid recovery. A new macroscopic mass flux equation is derived and it can be used to replace Darcy’s law for primary fluid recovery.

2. Asymptotic expansion of the governing equations for low-Mach-number flow

Pore-scale flow of a compressible fluid is governed by the continuity and compressible Navier–Stokes equations (Anderson 1995)

$$\frac{\partial \rho}{\partial t} + \nabla \cdot (\rho \mathbf{v}) = 0, \tag{2.1}$$

$$\rho \frac{\partial \mathbf{v}}{\partial t} + \rho \mathbf{v} \cdot \nabla \mathbf{v} = -\nabla p + \left(\mu_b + \frac{1}{3} \mu \right) \nabla (\nabla \cdot \mathbf{v}) + \mu \nabla^2 \mathbf{v}, \tag{2.2}$$

where \mathbf{v} , p , ρ are the velocity, pressure and density, and μ , μ_b are the shear and bulk viscosity of the fluid, respectively. Temperature change is assumed to be negligible. We follow Klainerman & Majda (1982) in making the governing equations dimensionless. Let v_{ref} be the magnitude of a reference fluid particle velocity, L_{ref} a reference length, and a reference time is defined as $t_{ref} = L_{ref}/v_{ref}$. The reference pressure and density are p_{ref} and ρ_{ref} , respectively. A reference speed of sound can be defined as $c_{ref} = \sqrt{p_{ref}/\rho_{ref}}$ (a constant factor is dropped for convenience; see Klainerman & Majda (1982)). We define dimensionless velocity, pressure, density, coordinates and time as $\bar{\mathbf{v}} = \mathbf{v}/v_{ref}$, $\bar{p} = p/p_{ref}$, $\bar{\rho} = \rho/\rho_{ref}$, $\bar{\mathbf{x}} = \mathbf{x}/L_{ref}$ and $\bar{t} = t/t_{ref}$. A global Mach number is defined as $M = v_{ref}/c_{ref}$, and it will be assumed small. A Reynolds number is defined as $Re = \rho_{ref} v_{ref} L_{ref}/\mu$. The dimensionless equations are

$$\frac{\partial \bar{\rho}}{\partial \bar{t}} + \bar{\nabla} \cdot (\bar{\rho} \bar{\mathbf{v}}) = 0, \tag{2.3}$$

$$\bar{\rho} \frac{\partial \bar{\mathbf{v}}}{\partial \bar{t}} + \bar{\rho} \bar{\mathbf{v}} \cdot \bar{\nabla} \bar{\mathbf{v}} = -\frac{1}{M^2} \bar{\nabla} \bar{p} + \frac{\mu_b/\mu + 1/3}{Re} \bar{\nabla} (\bar{\nabla} \cdot \bar{\mathbf{v}}) + \frac{1}{Re} \bar{\nabla}^2 \bar{\mathbf{v}}. \tag{2.4}$$

Using these equations and for inviscid isentropic flow, Klainerman & Majda (1982) have rigorously proved that, for given initial data, the linearized acoustics is a uniformly valid principal correction in the deviation of the compressible flow solution from the incompressible solution as the global Mach number $M \rightarrow 0$, i.e.

$$|\bar{\mathbf{v}} - (\bar{\mathbf{v}}^I + M \tilde{\mathbf{v}}^A)| \leq \Delta_5 M^2, \tag{2.5}$$

$$|\bar{p} - (\bar{p}_0 + M^2(\bar{p}^I + \tilde{p}^A))| \leq \Delta_6 M^3, \tag{2.6}$$

where $|\cdot|$ stands for the magnitude, and superscripts ‘I’ and ‘A’ stand for incompressible and acoustic quantities, respectively; $\bar{\mathbf{v}}^I = \lim_{M \rightarrow 0} \bar{\mathbf{v}}$ with $\bar{\mathbf{V}} \cdot \bar{\mathbf{v}}^I = 0$ is the incompressible solution at vanishing Mach number; $\Delta_5 > 0$, $\Delta_6 > 0$ are fixed constants, and \bar{p}_0 is a background thermodynamic pressure. This asymptotic result has been extended by Klein (1995) to non-isentropic flows and by Munz *et al.* (2003) and Munz, Dumbser & Rolle (2007) to the general heat-conducting viscous compressible Navier–Stokes equations. These asymptotic results have been used to construct efficient numerical schemes such as the multiple-pressure-variable method to overcome slow convergence, even failure, of fully compressible solvers for small-Mach-number flows (Klein 1995; Klein & Munz 1995; Bijl & Wesseling 1998; Bailly, Bogey & Juve 1999; Wesseling 2001; Munz *et al.* 2003, 2007).

The above asymptotic theory allows us to decompose a low-Mach-number flow into the sum of two fields, the limiting incompressible field $\bar{\mathbf{v}}^I$ and a linearized acoustic field $\bar{\mathbf{v}}^A$,

$$\bar{\mathbf{v}} = \bar{\mathbf{v}}^I + \bar{\mathbf{v}}^A. \tag{2.7}$$

For primary recovery, the outer boundary of the reservoir is non-penetrable. Thus, except for isolated dead pores, all pores in the reservoir are half-sealed, with the sealed ends located on the outer boundary or in the interior of the reservoir, and the open ends located at the wellbore where the fluid is being produced. Therefore, an incompressible velocity field does not contribute to the mass flow rate at the wellbore, since integration of the incompressibility condition over the connected pore space gives the corresponding volumetric flow rate at the wellbore as zero:

$$Q^I = \int_{\text{wellbore}} \mathbf{n} \cdot \mathbf{v}^I \, da = - \int_{\text{outer boundary}} \mathbf{n} \cdot \mathbf{v}^I \, da = 0, \tag{2.8}$$

where \mathbf{n} is the unit outward normal vector on the corresponding boundaries. Since the flow in half-sealed pores relies entirely on the volumetric expansion or compressibility of the fluid, the limiting incompressible velocity $\bar{\mathbf{v}}^I = \lim_{M \rightarrow 0} \bar{\mathbf{v}}$ must be identically zero in primary recovery, $\bar{\mathbf{v}}^I = 0$. For $\bar{\mathbf{v}}^I$ to be non-zero, the pores must have two open ends. Physically, an incompressible fluid cannot expand in volume; and in half-sealed pores, there is no fresh fluid to take the place of the volume in the pore space that would have been vacated by the produced fluid. In other words, to leading order, flow in primary recovery is completely characterized by the acoustic field $\bar{\mathbf{v}}^A$ (since $\bar{\mathbf{v}}^I = 0$), which is coupled to the density change of the fluid. Primary recovery is determined by how a fluid expands in volume in semi-sealed pores, not by how it is pushed out of the pores such as in a tube with open ends.

The acoustic velocity field $\bar{\mathbf{v}}^A$ can be further decomposed into the sum of an irrotational part $\bar{\mathbf{v}}_{IR}$ and a rotational part $\bar{\mathbf{v}}_{RT}$ using the Helmholtz decomposition theorem (Aris 1989; Leal 2010; Panton 2013),

$$\bar{\mathbf{v}}^A = \bar{\mathbf{v}}_{IR} + \bar{\mathbf{v}}_{RT}, \tag{2.9}$$

where the irrotational part is a potential flow and the rotational part is solenoidal (divergence-free):

$$\nabla \times \bar{\mathbf{v}}_{IR} = 0, \quad \bar{\mathbf{v}}_{IR} = \nabla \Phi, \tag{2.10}$$

$$\nabla \cdot \bar{\mathbf{v}}_{RT} = 0. \tag{2.11}$$

In the above, Φ is the scalar velocity potential for the irrotational part of the velocity. Thus, for primary recovery, $\bar{\mathbf{v}}^I = 0$, and the asymptotic results (2.5) and (2.6) suggest the following small-Mach-number expansions for the velocity and pressure:

$$\bar{\mathbf{v}} = \bar{\mathbf{v}}^A + O(M^2) = M \tilde{\mathbf{v}}_{RT} + M \tilde{\mathbf{v}}_{IR} + O(M^2), \tag{2.12}$$

$$\bar{p} - \bar{p}_0 = M^2 \tilde{p}_1 + M^2 \tilde{p}^A + O(M^3), \tag{2.13}$$

where $\bar{\mathbf{v}}_{RT} = M \tilde{\mathbf{v}}_{RT}$ and $\bar{\mathbf{v}}_{IR} = M \tilde{\mathbf{v}}_{IR}$. The pressure $\bar{p}_1 = M^2 \tilde{p}_1$ is the Lagrangian multiplier associated with the solenoidal field $\tilde{\mathbf{v}}_{RT}$ to ensure that the incompressibility condition for $\tilde{\mathbf{v}}_{RT}$ is satisfied. The pressure \tilde{p}_1 is thus a hydrodynamic pressure induced by the solenoidal field $\tilde{\mathbf{v}}_{RT}$ and it is not described by the equation of state. The necessity to include \tilde{p}_1 in the pressure expansion has been discussed by Klein (1995) and Munz *et al.* (2003, 2007). The estimates (2.5) and (2.6) guarantee the convergence of the series (2.12) and (2.13) in the limit $M \rightarrow 0$. Density can be similarly expanded as

$$\bar{\rho} = 1 + M^2 \tilde{\rho}_2 + O(M^4). \tag{2.14}$$

Density change is only related to the acoustic pressure $\bar{p}^A = M^2 \tilde{p}^A$ via the equation of state

$$\tilde{p}^A = \tilde{\rho}_2. \tag{2.15}$$

When the expansions (2.12) and (2.13) are substituted into the governing equations, to leading order we obtain the following equations for the irrotational field:

$$\frac{\partial \tilde{\rho}_2}{\partial \tilde{t}} + \bar{\nabla} \cdot \tilde{\mathbf{v}}_{IR} = 0, \tag{2.16}$$

$$\frac{\partial \tilde{\mathbf{v}}_{IR}}{\partial \tilde{t}} = -\bar{\nabla} \tilde{p}^A + \frac{\mu_b/\mu + 4/3}{Re_{AC}} \bar{\nabla} (\bar{\nabla} \cdot \tilde{\mathbf{v}}_{IR}), \tag{2.17}$$

$$\tilde{p}^A = \tilde{\rho}_2, \tag{2.18}$$

where the fast-time variable $\tilde{t} = \bar{t}/M = t/t_{ref,AC}$, with $t_{ref,AC} = L_{ref}/c_{ref}$ being the acoustic time scale; and the acoustic Reynolds number $Re_{AC} = \rho_{ref} c_{ref} L_{ref} / \mu$, which is related to the Reynolds number by $Re = M Re_{AC}$. The leading-order solenoidal field equations are

$$\bar{\nabla} \cdot \tilde{\mathbf{v}}_{RT} = 0, \tag{2.19}$$

$$\frac{\partial \tilde{\mathbf{v}}_{RT}}{\partial \tilde{t}} = -\bar{\nabla} \tilde{p}_1 + \frac{1}{Re} \bar{\nabla}^2 \tilde{\mathbf{v}}_{RT}. \tag{2.20}$$

In the acoustic literature, the irrotational field and the solenoidal field are called the longitudinal mode and the transverse mode, respectively (Morse & Ingard 1968; Pierce 1981).

It is noted that the solenoidal field is absent in the leading-order irrotational velocity equations (2.16)–(2.18). The irrotational velocity, however, should not be expected to satisfy the no-slip condition on a solid boundary. The solenoidal field $\tilde{\mathbf{v}}_{RT}$ is induced by the irrotational velocity $\tilde{\mathbf{v}}_{IR}$ at the boundary so that the no-slip condition for the overall velocity $\bar{\mathbf{v}}^A = \tilde{\mathbf{v}}_{RT} + \tilde{\mathbf{v}}_{IR}$ on the pore wall is satisfied:

$$\tilde{\mathbf{v}}_{RT} = -\tilde{\mathbf{v}}_{IR}. \tag{2.21}$$

For primary recovery, the solenoidal field $\tilde{\mathbf{v}}_{RT}$ does not generate a net flow rate (see (2.8)).

It is noted that mode decomposition of the linear acoustic field has been used for a long time and it was examined theoretically in detail by Lagerstrom, Cole & Trilling (1949) and Wu (1956). However, there is one major difference between these earlier works and the one presented here: in the earlier studies, the pressure \tilde{p}_1 in the solenoidal field momentum equation (2.20) has been set to zero identically, $\tilde{p}_1 = 0$ (Lagerstrom *et al.* 1949; Wu 1956; Morse & Ingard 1968; Pierce 1981; Temkin 1981; Friend & Yeo 2011). However, without this induced pressure, which serves as a Lagrangian multiplier to enforce the incompressibility condition for the solenoidal field, the solenoidal equations (2.19) and (2.20) are, in general, overdetermined, as there would be four equations for three unknowns (the three velocity components). Thus, in the absence of \tilde{p}_1 , except for a few special cases, the set of equations (2.19) and (2.20) is likely to give rise to solutions that are internally incompatible due to overconstraint. In fact, a key result of the asymptotic theory of Klainerman & Majda (1982) is the splitting of the pressure into the sum of a thermodynamic pressure, a hydrodynamic pressure and an acoustic pressure for small-Mach-number flows. The distinct multiple roles that pressure plays physically in the small-Mach-number limit of a compressible flow and the necessity to include \tilde{p}_1 in the pressure expansion have been discussed in detail in Klein (1995), Klein & Munz (1995) and Munz *et al.* (2003, 2007). These results form the basis for the multiple-pressure-variable numerical method for small-Mach-number flows (Klein 1995; Klein & Munz 1995; Bijl & Wesseling 1998; Bailly *et al.* 1999; Klein *et al.* 2001; Wesseling 2001; Munz *et al.* 2003, 2007).

3. The damped wave equation for density and its asymptotic form at large times

For primary fluid recovery, integration of the continuity equation (2.1) in the entire interconnected pore space gives the mass flow rate at the wellbore as

$$\dot{m} = - \int_{\text{pore space}} \frac{\partial \rho}{\partial t} dV, \quad (3.1)$$

where the property that the outer boundary is non-penetrable has been used. Thus, density change in the pore space determines the mass production rate at the wellbore. Density change appears only in the equations (2.16)–(2.18) for the irrotational field, which leads to a decoupled damped wave equation for the density:

$$\frac{\partial^2 \tilde{\rho}_2}{\partial \tilde{t}^2} = \bar{\nabla}^2 \tilde{\rho}_2 + \frac{\mu_b/\mu + 4/3}{Re_{AC}} \frac{\partial}{\partial \tilde{t}} \bar{\nabla}^2 \tilde{\rho}_2. \quad (3.2)$$

This equation is based on the fast acoustic time scale \tilde{t} . The dimensional form of the damped wave equation is

$$\frac{\partial^2 \rho}{\partial t^2} = c_{ref}^2 \nabla^2 \rho + D_{\rho,0} \frac{\partial}{\partial t} \nabla^2 \rho, \quad (3.3)$$

where

$$D_{\rho,0} = \frac{\mu_b + 4\mu/3}{\rho_{ref} \nu_{ref}} = (\mu_b/\mu + 4/3) \nu_{ref}, \quad (3.4)$$

with $\nu_{ref} = \mu/\rho_{ref}$ being the kinematic viscosity. Here $D_{\rho,0}$ is a damping coefficient, as the last term on the right-hand side of (3.3) represents viscous damping of the acoustic (density) waves; $D_{\rho,0}$ is also the self-diffusion coefficient of the fluid, as the damping

stems from the self-diffusion of the fluid mass due to a local density gradient. When the bulk viscosity is zero as in the Stokes hypothesis, $D_{\rho,0} = 4\nu_{ref}/3$. This result is consistent with the kinetic theory of gases, which shows that the self-diffusivity of a gas is proportional to the momentum diffusion coefficient ν (Hirschfelder, Curtiss & Bird 1954). Damping presented by the last term on the right-hand side of (3.3) is also called sound absorption, as the acoustic waves are absorbed by the bulk of the fluid. In the absence of a source for continuous excitation, an acoustic wave is expected to be absorbed by the fluid as well as the boundaries and damped out over large times (here ‘large’ is relative to the acoustic time scale). The linear damped wave equation (3.3), called the Stokes equation by Rayleigh (1945), is well known in the acoustic literature and it has appeared in many textbooks (e.g. Morse & Ingard 1968; Temkin 1981).

When the damped wave equation (3.2) is expressed in terms of the slow time variable $\bar{t} = M\tilde{t}$, which is suitable for large times, we have

$$M^2 \frac{\partial^2 \tilde{\rho}_2}{\partial \tilde{t}^2} = \bar{\nabla}^2 \tilde{\rho}_2 + M^2 \frac{\mu_b/\mu + 4/3}{Re} \frac{\partial}{\partial \tilde{t}} \bar{\nabla}^2 \tilde{\rho}_2, \tag{3.5}$$

where the relation $Re = MRe_{AC}$ has been used. Thus, when viewed on the large time scale, to leading order in Mach number,

$$\bar{\nabla}^2 \tilde{\rho}_2 = 0. \tag{3.6}$$

This is the equation for $\bar{t} \rightarrow \infty$ that corresponds to the final equilibrium state. At the next order, i.e. for finite \bar{t} , we have a diffusion equation,

$$\frac{\partial^2 \tilde{\rho}_2}{\partial \tilde{t}^2} = \frac{\mu_b/\mu + 4/3}{Re} \frac{\partial}{\partial \tilde{t}} \bar{\nabla}^2 \tilde{\rho}_2. \tag{3.7}$$

Consider an initial value problem starting from the state of rest. Then, the initial condition $\tilde{t} = 0: \partial \tilde{\rho}_2 / \partial \tilde{t} = 0$ can be approximated as $\bar{t} = 0: \partial \tilde{\rho}_2 / \partial \tilde{t} = 0$ for the diffusion equation (3.7) if the acoustic waves are damped rapidly when measured on the large time scale \bar{t} . Integration of the diffusion equation (3.7) yields the standard diffusion equation

$$\frac{\partial \tilde{\rho}_2}{\partial \tilde{t}} = \frac{\mu_b/\mu + 4/3}{Re} \bar{\nabla}^2 \tilde{\rho}_2. \tag{3.8}$$

Thus, at large times, the density wave becomes purely diffusive, controlled by diffusion with a diffusive velocity scale $\nu_{ref} = D_{\rho,0}/L_{ref}$. The Reynolds number is then $Re = \mu_b/\mu + 4/3$, and the dimensionless diffusion equation (3.8) becomes

$$\frac{\partial \tilde{\rho}_2}{\partial \tilde{t}} = \bar{\nabla}^2 \tilde{\rho}_2, \tag{3.9}$$

where $\bar{t} = t/t_{ref} = D_{\rho,0}t/L_{ref}^2$. Once the density is solved from the diffusion equation (3.9), the irrotational velocity can be obtained from the continuity equation (2.16) and the solenoidal field from solving (2.19) and (2.20).

It should be noted that, with an error of the order of $O(M^4)$, equation (3.9) can be written as

$$\frac{\partial \bar{\rho}}{\partial \bar{t}} = \bar{\nabla}^2 \ln \bar{\rho}. \tag{3.10}$$

In dimensional form,

$$\frac{\partial \rho}{\partial t} = \nabla \cdot (D_\rho \nabla \rho), \tag{3.11}$$

where

$$D_\rho = (\mu_b/\mu + 4/3)\nu, \quad (3.12)$$

with $\nu = \mu/\rho$ being the variable kinematic viscosity, is a density-dependent diffusion coefficient. It can be easily shown from (3.11) and the continuity equation that the mass flux of the irrotational field $\dot{\mathbf{m}}_{IR} = \rho\mathbf{v}_{IR}$ for primary recovery is given by a Fick's law type of relation,

$$\dot{\mathbf{m}}_{IR} = -D_\rho \nabla \rho. \quad (3.13)$$

Since the solenoidal field does not contribute to the mass flow rate in primary recovery, the irrotational mass flux $\dot{\mathbf{m}}_{IR}$ is also the pore-scale mass flux $\dot{\mathbf{m}} = \rho\mathbf{v}$ for primary recovery, i.e. $\dot{\mathbf{m}} = \dot{\mathbf{m}}_{IR}$.

The above analysis shows that, at large times, density in the pore space diffuses according to the diffusion equation (3.11) with the diffusion coefficient given by (3.12). We emphasize that the diffusive time scale $t_{ref} = L_{ref}^2/D_{\rho,0}$ is always much larger than the acoustic time scale $t_{ref,AC} = L_{ref}/c_{ref}$; and 'large' or 'long' time is measured relative to the acoustic time scale. The density diffusion equation (3.11) is derived from an asymptotic analysis of the compressible Navier–Stokes equations at low Mach numbers, and it is the fundamental pore-scale transport equation from which upscaling can be performed.

For a semi-sealed cylindrical pore with a radius R and length L , Chen & Shen (2018a,b) obtained the complete solution for drainage flow using the linearized damped wave equation (3.3). A prominent feature of the pore-scale flow is that density relaxes quickly in the transverse direction after the start-up and density becomes uniform in the tube cross-section. The velocity field satisfies the no-slip condition and the fluid production rate at large times is given by

$$\dot{m}_e(t) = 2M_L \frac{D_{\rho,0}}{L^2} \sum_{n=0}^{\infty} \exp \left[-\frac{(2n+1)^2 \pi^2 D_{\rho,0} t}{4L^2} \right], \quad (3.14)$$

where $M_L = \pi R^2 L(\rho_i - \rho_e)$ is the amount of producible fluid for the given density drop; and ρ_i and ρ_e are the initial density and exit density, respectively. The same result can be obtained by solving the linearized density diffusion equation (3.9). Clearly, the fluid production rate exhibits a slip-like behaviour as it is proportional to R^2 . The fluid production rate is proportional to the fluid's kinematic viscosity instead of the reciprocal of the kinematic viscosity as provided by the classical Poiseuille's law. These pore-scale results are indicative of the invalidity of the Poiseuille–Darcy framework for flow in primary recovery at the pore scale, and consequently at the macroscale.

4. Macroscopic equations for primary recovery

At the pore scale, density change is controlled by self-diffusion and it obeys the diffusion equation (3.11). Thus, to compute the fluid production rate for primary recovery using the macroscopic equation (A4) given in appendix A, we only need to upscale the density diffusion equation (3.11) subject to the zero-mass-flux condition on the pore wall,

$$\mathbf{n} \cdot \nabla \rho = 0. \quad (4.1)$$

The spatial deviation of the density, $\rho - \langle \rho \rangle^f$, as defined in Whitaker (1986) with $\langle \rho \rangle^f$ being the intrinsic average of the density (appendix A), also satisfies the boundary condition (4.1).

The problem of upscaling a diffusion equation with a heterogeneous reaction in porous media has been studied in detail by Whitaker (1999) and more recently by Lugo-Mendez *et al.* (2015). Other works on upscaling of a diffusion equation using the same methodology include, but are not limited to, Wood & Whitaker (1997, 1999), Valdes-Parada *et al.* (2009), Valdes-Parada & Aguilar-Madera (2011), Valdes-Parada, Aguilar-Madera & Alvarez-Ramirez (2011), Benitez-Olivares, Valdes-Parada & Saucedo-Castaneda (2016), Santos-Sanchez, Valdes-Parada & Chirino (2016) and Valdes-Parada, Lasseux & Whitaker (2017). In the absence of reaction, the microscopic-scale diffusion problem studied by Whitaker (1999) and Lugo-Mendez *et al.* (2015) is exactly the same as the diffusion equation (3.11) with the no-penetration condition on the fluid–solid surface (4.1). Thus, the upscaled density diffusion equation for the present problem is a special case of the upscaled diffusion equation of Lugo-Mendez *et al.* (2015, equation (41)), which takes the form

$$\frac{\partial \langle \rho \rangle^f}{\partial t} = \nabla \cdot (D_{\langle \rho \rangle^f} \nabla \langle \rho \rangle^f), \tag{4.2}$$

where the diffusion coefficient is valued at the averaged density,

$$D_{\langle \rho \rangle^f} = \frac{\mu_b + 4\mu/3}{\langle \rho \rangle^f}. \tag{4.3}$$

The upscaled equation (4.2) is derived under the condition that the closure problem for the spatial deviation of the density is local, periodic, quasi-steady and linear. Under this condition and in the absence of reaction, the local closure problem for the spatial deviation of the density (equations (18a–e) of Lugo-Mendez *et al.* (2015)), is homogeneous when subject to the no-penetration boundary condition and zero initial deviation. Thus, the spatial deviation of the density is identically zero. The specific time- and length-scale constraints corresponding to the above condition for simplifying the closure problem have been examined in detail by Lugo-Mendez *et al.* (2015), which become (note that the so-called Thiele modulus for the closure problem is zero in the absence of reaction)

$$\left. \begin{aligned} \ell_\gamma &\ll r_0 \ll L, \\ \frac{\ell_\gamma}{L} &\ll 1, \\ 1 &\ll \frac{D_{\rho,0} t^*}{\ell_\gamma^2}. \end{aligned} \right\} \tag{4.4}$$

In (4.4), ℓ_γ is the characteristic length for the fluid phase, which can be taken as the pore throat diameter; r_0 is the characteristic size of the averaging volume; L is the characteristic length of the porous system, which can be taken as the size of the reservoir; and t^* is a characteristic time for the fluid production. The characteristic time for primary recovery is the diffusive time scale $L^2/D_{\rho,0}$; thus, the third condition in (4.4) coincides with the second condition. The diffusion coefficient (4.3) is valued at the mean density $\langle \rho \rangle^f$ of the averaging cell. This can be obtained by a Taylor-series expansion and neglecting the nonlinear terms under the local theory, as shown by Lugo-Mendez *et al.* (2015). In cases where the length-scale constraints prevent such a linearization, Lugo-Mendez *et al.* (2015) have also developed an iterative procedure for the nonlinear closure problem.

The new diffusion equation (4.2) for $\langle \rho \rangle^f$ can be compared to the classical diffusion equation (A 6) for $\langle \rho \rangle^f$ based on Darcy's law listed in appendix A. The diffusion coefficient $D_{\langle \rho \rangle^f}$ for (4.2) differs significantly, both physically and magnitude-wise, from the classical diffusion coefficient D_{Darcy} in (A 6) given by (A 7), $D_{Darcy} = \kappa c_T^2 \langle \rho \rangle^f / (\mu \phi)$, with κ , ϕ , c_T being the permeability and porosity of the porous medium and the isothermal speed of sound of the fluid, respectively. The diffusion coefficient $D_{\langle \rho \rangle^f}$ is directly related to the self-diffusion coefficient of the fluid,

$$D_{11} = (\mu_b / \mu + 4/3)\nu. \quad (4.5)$$

When the bulk viscosity is zero, $D_{11} = 1.33\nu$ for a dilute gas (Hirschfelder *et al.* 1954). The appearance of the self-diffusion coefficient in the pore-scale fluid density diffusion equation (3.11) as well as the upscaled fluid density diffusion equation (4.2) for the intrinsic average density $\langle \rho \rangle^f$ is natural and expected, as the density diffusion equation describes the mass transport process in the diffusion-dominated flow regime. On the other hand, D_{Darcy} is inversely proportional to the self-diffusion coefficient D_{11} , since D_{Darcy} is inversely proportional to the kinematic viscosity ν . Darcy's law is only appropriate for incompressible flows and it is irrelevant to the self-diffusion process. Therefore, the classical diffusion coefficient D_{Darcy} cannot be the correct diffusion coefficient for the intrinsic average density $\langle \rho \rangle^f$.

In addition, the magnitude of $D_{\langle \rho \rangle^f}$ can be several orders of magnitude higher than D_{Darcy} . If we evaluate the diffusivities $D_{\langle \rho \rangle^f}$ and D_{Darcy} for methane at typical shale conditions at temperature 80 °C and pressure of 25 MPa (appendix B), we have $D_{Darcy} = 4.53 \times 10^{-8} \text{ m}^2 \text{ s}^{-1}$ when the porosity is $\phi = 0.1$ and the permeability is one nanodarcy ($\kappa \approx 10^{-21} \text{ m}^2$); while $D_{\langle \rho \rangle^f} = 4.82 \times 10^{-5} \text{ m}^2 \text{ s}^{-1}$. Thus, for methane in shale, $D_{\langle \rho \rangle^f}$ is three orders of magnitude higher than D_{Darcy} . At a lower pressure, the difference between these two diffusion coefficients becomes even larger, since, as the pressure is decreased, $D_{\langle \rho \rangle^f}$ increases while D_{Darcy} decreases.

To find the mass flux \mathbf{J} , which is the mass flow rate per unit porous medium area, the density diffusion equation (4.2) needs to be written in the form

$$\frac{\partial m}{\partial t} + \nabla \cdot \mathbf{J} = 0, \quad (4.6)$$

where m is fluid mass per unit porous medium volume, i.e. the superficial average density $\langle \rho \rangle$, which is related to intrinsic averaged density $\langle \rho \rangle^f$ by $\langle \rho \rangle = \phi \langle \rho \rangle^f$ (appendix A). Thus,

$$\frac{\partial \langle \rho \rangle}{\partial t} - \nabla \cdot \left(\phi \frac{\mu_b + 4\mu/3}{\langle \rho \rangle} \nabla \langle \rho \rangle \right) = 0. \quad (4.7)$$

Equation (4.7) is the effective (i.e. homogenized) medium equation, which shows that, in the effective medium, mass (density) diffuses with a mass diffusion coefficient

$$D_m = \phi \frac{\mu_b + 4\mu/3}{\langle \rho \rangle}. \quad (4.8)$$

Clearly, D_m depends on the porosity, but not on the permeability. The mass flux \mathbf{J} is given by

$$\mathbf{J} = -D_m \nabla \langle \rho \rangle, \quad (4.9)$$

which is also independent of permeability. Permeability is a property introduced by Darcy's law for incompressible flows and it plays no role in determining the mass flow rate in primary recovery. Thus, Darcy's law should be replaced by the mass flux equation (4.9) for primary fluid recovery.

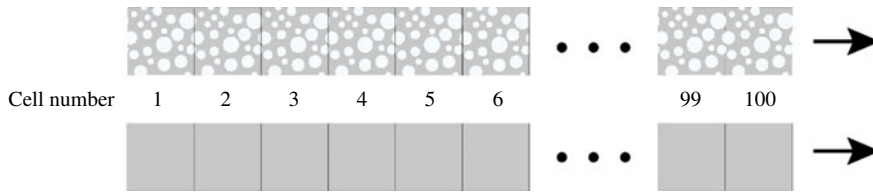


FIGURE 3. Top: Microscale simulation for density in drainage flow (primary recovery) with 100 horizontally repeated identical unit cells. The solid circles (totalling 49 for $\phi = 0.5840$) are randomly distributed in the unit cell. Bottom: Macroscale effective medium simulation for density distribution. Three porosities $\phi = 0.5840, 0.4630, 0.3202$ are considered.

5. Comparison of macroscale equation with pore-scale simulation

In this section, we solve the upscaled and the microscale density diffusion equations for drainage of a compressible fluid from a semi-sealed two-dimensional porous medium channel and compare the average density distributions (figure 3). The porous medium is made of 100 identical unit cells with a compressible fluid saturating the pore space with an initial density ρ_i . The solids in a unit cell with a size of $0.02 \text{ m} \times 0.02 \text{ m}$ are randomly distributed circles with various diameters between 0.0004 m and 0.0025 m obeying the normal size distribution (several such random generated patterns have been tested and they produce the same cell averaged densities). The left end of the channel is sealed while the right end is opened at $t = 0$, with an exit density $\rho_e < \rho_i$. We solve the microscale density diffusion equation (3.11) in the pore space, together with the no-penetration condition (4.1) imposed on the solid surfaces, including the channel walls. We then compute the average density in each unit cell and compare the result to the corresponding macroscale density. The macroscale density is obtained by solving the effective medium density diffusion equation (4.7) subject to the no-penetration condition on the channel walls. Both calculations are carried out using COMSOL (COMSOL 2016). In these computations, $\rho_i = 1 \text{ kg m}^{-3}$, $\rho_e = 0.9 \text{ kg m}^{-3}$, $\mu = 10^{-3} \text{ Pa s}$, $r_0 = 0.02 \text{ m}$, $L = 2 \text{ m}$ and three porosities $\phi = 0.5840, 0.4630, 0.3202$ have been used. A large viscosity value is chosen in order to shorten the computational time required for draining out the fluid from the channel. Convergence tests have been conducted by mesh refinements.

Figure 4 shows the local density distributions for each system for the case $\phi = 0.5840$ in three segments of the channel at time $t = 1000 \text{ s}$, for cells 6–15, cells 46–55 and cells 85–94. It is observed that the microscale density distribution in each unit cell is fairly uniform despite the presence of the solid fractions, and there is little difference between the microscale and macroscale densities in these three segments. Figure 5 shows a specific comparison of the cell-averaged dimensionless density ρ_{avg}/ρ_i for these two systems for cells 10, 50 and 90 (marked as A, B and C, respectively). For the microscale model, the average density $\rho_{avg,mic}$ is the intrinsically averaged density in the unit cell; while for the macroscale model, $\rho_{avg,mac}$ is averaged over the entire unit cell area since the medium is homogenized. The relative error of the cell-averaged density between these two models, defined as $|\rho_{avg,mac} - \rho_{avg,mic}|/\rho_{avg,mic}$, is plotted against time for each of these three cells in figure 6(a). The maximum relative errors for these three cells (A, B and C) are 0.6%, 0.4% and 0.1%, respectively. Similarly, for $\phi = 0.4630$, the maximum relative errors for these three cells are 0.65%, 0.45% and 0.15%, respectively, as shown in

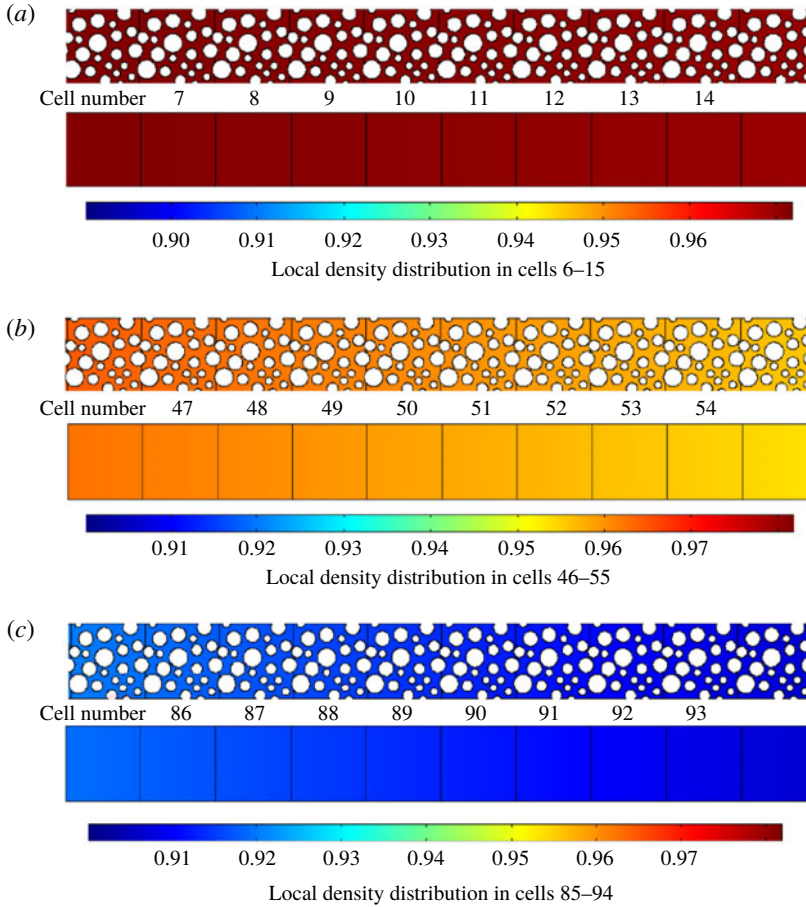


FIGURE 4. (Colour online) Computed local density distributions in the various cells indicated for the two systems, microscale (top) and macroscale (effective medium) (bottom) at time $t = 1000$ s, for $\phi = 0.5840$ and $\mu = 10^{-3}$ Pa s. Initial density $\rho_i = 1$ kg m $^{-3}$ and exit density $\rho_e = 0.9$ kg m $^{-3}$.

figure 6(b). For $\phi = 0.3202$, the maximum relative errors for these three cells are 1%, 0.7% and 0.3%, respectively (figure 6c). This range of relative error is acceptable for many practical applications. Together, these comparisons provide a numerical validation of the upscaled density equation.

6. Conclusions

The work reported in this study shows that the macroscopic equation for primary fluid recovery is fundamentally different from Darcy's law. The key reason for this difference is that primary fluid recovery is entirely driven by the fluid's volumetric expansion; as a result, the corresponding incompressible limit of the velocity is identically zero. Since Darcy's law arises from the upscaling of this incompressible limit velocity, it then becomes irrelevant to primary recovery. Instead, Darcy's law should be replaced by the mass flux equation (4.9) for such a process. In particular, the mass production rate depends on the porosity, but not on the permeability, of

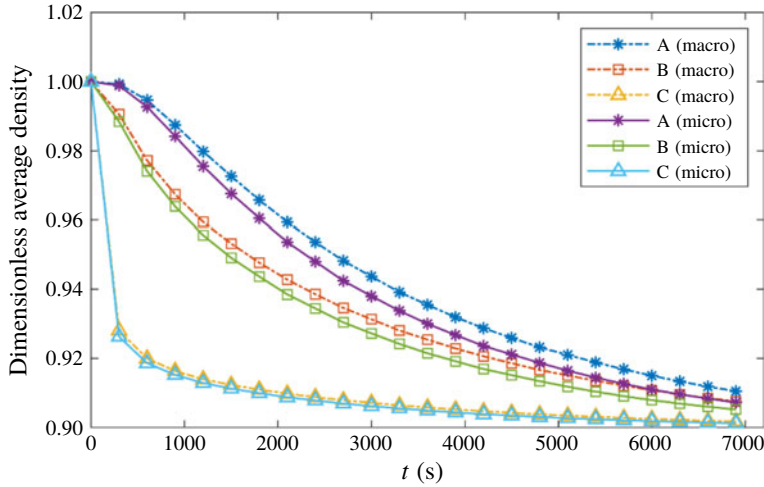


FIGURE 5. (Colour online) Comparison of the dimensionless average density for the three cells (A, B and C) computed from the macroscale equation and the microscale equation, for $\phi = 0.5840$.

the porous medium. The implication of this result can be significant for hydrocarbon recovery and possibly for other applications.

Acknowledgements

We thank Professor M. Hermann for bringing the work of R. Klein to our attention and the reviewers for their helpful suggestions.

Appendix A. Classical macroscopic equations

Consider the motion of a single-phase compressible fluid in a fully saturated isotropic homogeneous and rigid porous medium. The superficial averages of the fluid density ρ and velocity \mathbf{v} are defined in terms of the porous medium volume as

$$\langle \rho \rangle = \frac{1}{V} \int_{V_f} \rho \, dv, \quad \langle \mathbf{v} \rangle = \frac{1}{V} \int_{V_f} \mathbf{v} \, dv, \tag{A 1a,b}$$

where V , V_f are the local volumes of the porous medium and the fluid, respectively. The superficial averages are related to the intrinsic phase averages, denoted by superscript ‘f’ and defined in terms of the fluid volume, by the simple relations

$$\langle \rho \rangle = \phi \langle \rho \rangle^f, \quad \langle \mathbf{v} \rangle = \phi \langle \mathbf{v} \rangle^f, \tag{A 2a,b}$$

where $\phi = V_f/V$ is the porosity or volume fraction of the fluid phase. The superficial average velocity $\langle \mathbf{v} \rangle$ is also known as the specific discharge, which is the volumetric flow rate per unit area of the porous medium. The macroscopic-level continuity equation expressed for unit medium volume, which for a rigid porous medium, $\phi = \text{const.}$, can be written (Lasseux *et al.* 2014) as

$$\frac{\partial}{\partial t} (\phi \langle \rho \rangle^f) + \nabla \cdot (\langle \rho \rangle^f \langle \mathbf{v} \rangle) = 0. \tag{A 3}$$

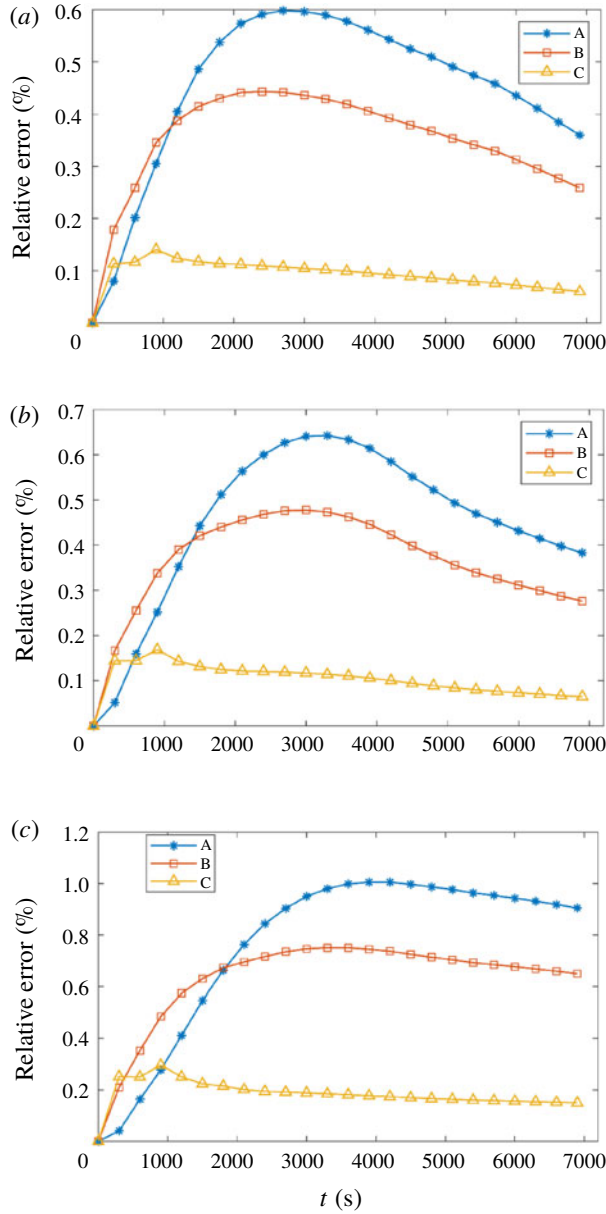


FIGURE 6. (Colour online) Relative error $|\rho_{avg,mac} - \rho_{avg,mic}|/\rho_{avg,mic}$ versus time for the three representative cells: (a) $\phi = 0.5840$, (b) $\phi = 0.4630$ and (c) $\phi = 0.3202$.

In primary fluid recovery, the outer boundary of the reservoir is non-penetrable and the inner boundary, for example a wellbore, is where the fluid is produced (figure 1). Integrating the continuity equation (A 3) over the entire reservoir volume and applying the divergence theorem gives the mass flow rate (production rate) at the wellbore as

$$\dot{m}_{primary} = \int_{exit} \langle \rho \rangle^f \mathbf{n} \cdot \langle \mathbf{v} \rangle da = -\frac{\partial}{\partial t} \int_{reservoir} \phi \langle \rho \rangle^f dv = -\frac{\partial}{\partial t} \int_{reservoir} \langle \rho \rangle dv, \quad (A 4)$$

where \mathbf{n} is the unit outward normal on the respective boundary. The integral on the right-hand side of (A 4) is the fluid mass in the reservoir, and (A 4) simply states that the rate of fluid produced at the wellbore is the time rate of decrease of the fluid mass in the reservoir. Equation (A 4) shows that density change is the most fundamental variable for primary fluid recovery. This result was well recognized a long time ago by Muskat (1937) in his pioneering work on flow in porous media, as he formulated his macroscopic governing equations using density change instead of pressure change almost exclusively. In the classical approach, Darcy's law (Darcy 1856; Bear 1972; Whitaker 1986)

$$\langle \mathbf{v} \rangle = -\frac{\kappa}{\mu} \nabla \langle \rho \rangle^f \quad (\text{A } 5)$$

is used to derive the governing equation for the density change at the macroscopic level. In (A 5), κ is the permeability and μ is the fluid's shear viscosity. Substituting (A 5) into (A 3) yields

$$\frac{\partial \langle \rho \rangle^f}{\partial t} = \nabla \cdot (D_{\text{Darcy}} \nabla \langle \rho \rangle^f), \quad (\text{A } 6)$$

with the diffusion coefficient

$$D_{\text{Darcy}} = \frac{\kappa c_T^2}{\mu \phi} \langle \rho \rangle^f, \quad (\text{A } 7)$$

where $c_T^2 = \partial \langle p \rangle^f / \partial \langle \rho \rangle^f|_T$ is the square of the isothermal speed of sound in the fluid.

Appendix B. Methane properties

The following properties of methane at 80 °C and 25 MPa, typical for shale formation, are taken from <http://www.peacesoftware.de/einigerwerte/methane.html>: $\mu = 1.99 \times 10^{-5}$ Pa s, $\mu_b = 6.368 \times 10^{-3}$ Pa s, $\rho = 136.78$ kg m⁻³, $c = 584$ m s⁻¹. In particular, the bulk viscosity for methane is estimated to be 320 times its shear viscosity at 80 °C (Cramer 2012).

REFERENCES

- ALAZARD, T. 2006 Low Mach number limit of the full Navier–Stokes equations. *Arch. Rat. Mech. Anal.* **180** (1), 1–73.
- ANDERSON, J. D. JR 1995 *Computational Fluid Dynamics*. McGraw-Hill.
- ARIS, R. 1989 *Vectors, Tensors, and the Basic Equations of Fluid Mechanics*. Dover.
- AURIAULT, J. L. 1987 Nonsaturated deformable porous media: quasistatics. *Trans. Porous Med.* **2**, 405–464.
- BAILLY, C., BOGEY, C. & JUVE, D. 1999 Computation of flow noise using source terms in linearized Euler equations. *AIAA J.* **37**, 409–416.
- BEAR, J. 1972 *Dynamics of Fluids in Porous Media*. American Elsevier.
- BENITEZ-OLIVARES, G., VALDES-PARADA, F. & SAUCEDO-CASTANEDA, J. 2016 Derivation of an upscaled model for mass transfer and reaction for non-food starch conversion to bioethanol. *Intl J. Chem. Reactor Engng* **14** (6), 1115–1148.
- BIJL, H. & WESSELING, P. 1998 A unified method for computing incompressible and compressible flows in boundary-fitted coordinates. *J. Comput. Phys.* **141**, 153–173.
- CHEN, K. P. & SHEN, D. 2018a Drainage flow of a viscous compressible fluid from a small capillary with a sealed end. *J. Fluid Mech.* **839**, 621–643.
- CHEN, K. P. & SHEN, D. 2018b Mechanism of fluid production from the nanopores of shale. *Mech. Res. Commun.* **88**, 34–39.

- COMSOL. 2016 Multiphysics® Modeling Software. COMSOL, Burlington, MA. www.comsol.com.
- CRAMER, M. S. 2012 Numerical estimates for the bulk viscosity of ideal gases. *Phys. Fluids* **24**, 066102.
- DAKE, L. P. 1978 *Fundamentals of Reservoir Engineering*. Elsevier.
- DANCHIN, R. 2001 Global existence in critical spaces for flows of compressible viscous and heat-conductive gases. *Arch. Rat. Mech. Anal.* **160** (1), 1–39.
- DANCHIN, R. 2002 Zero Mach number limit in critical spaces for compressible Navier–Stokes equations. *Ann. Sci. École Norm. Sup.* **35** (1), 27–75.
- DANCHIN, R. 2005 Low Mach number limit for viscous compressible flows. *Math. Modeling Numer. Anal.* **39** (3), 459–475.
- DARCY, H. 1856 *Les Fontaines Publiques de la Ville de Dijon*. Librairie des Corps Impériaux des Ponts et Chaussées et des Mines.
- DESJARDINS, B. & GRENIER, E. 1999 Low Mach number limit of viscous compressible flows in the whole space. *Proc. R. Soc. Lond. A* **455** (1986), 2271–2279.
- DESJARDINS, B., GRENIER, E., LIONS, P.-L. & MASMOUDI, N. 1999 Incompressible limit for solutions of the isentropic Navier–Stokes equations with Dirichlet boundary conditions. *J. Math. Pures Appl.* **78** (5), 461–471.
- DESJARDINS, B. & LIN, C.-K. 1999 A survey of the compressible Navier–Stokes equations. *Taiwanese J. Math.* **3** (2), 123–137.
- EBIN, D. G. 1977 The motion of slightly compressible fluids viewed as a motion with strong constraining force. *Ann. Math.* **105** (1), 141–200.
- EBIN, D. G. 1982 Motion of slightly compressible fluids in a bounded domain. Part I. *Commun. Pure Appl. Maths* **35** (4), 451–485.
- FEIREISL, E. & NOVOTNY, A. 2009 *Singular Limits in Thermodynamics of Viscous Fluids*. Birkhäuser.
- FRIEND, J. & YEO, L. Y. 2011 Microscale acoustofluidics: microfluidics driven via acoustics and ultrasonics. *Rev. Mod. Phys.* **83** (4), 647–704.
- HIRSCHFELDER, J. O., CURTISS, C. F. & BIRD, R. B. 1954 *Molecular Theory of Gases and Liquids*. Wiley.
- KELLER, J. B. 1980 Darcy’s law for flow in porous media and the two-space method. In *Nonlinear Partial Differential Equations in Engineering and Applied Science* (ed. R. L. Sternberg, A. J. Kalinowski & J. S. Papadakis), vol. 54, pp. 429–443. Dekker.
- KLAINERMAN, S. & MAJDA, A. 1981 Singular limits of quasilinear hyperbolic systems with large parameters and the incompressible limit of compressible fluids. *Commun. Pure Appl. Maths* **34** (4), 481–524.
- KLAINERMAN, S. & MAJDA, A. 1982 Compressible and incompressible fluids. *Commun. Pure Appl. Maths* **35** (5), 629–651.
- KLEIN, R. 1995 Semi-implicit extension of a Godunov-type scheme based on low Mach number asymptotics. Part I. One-dimensional flow. *J. Comput. Phys.* **121** (2), 213–237.
- KLEIN, R., BOTTA, N., SCHNEIDER, T., MUNZ, C. D., ROLLER, S., MEISTER, A., HOFFMANN, L. & SONAR, T. 2001 Asymptotic adaptive methods for multi-scale problems in fluid mechanics. *J. Engng Maths* **39** (1–4), 261–343.
- KLEIN, R. & MUNZ, C. D. 1995 The multiple pressure variables (MPV) for the numerical approximation of weakly compressible fluid flow. In *Proceedings of Numerical Modelling in Continuum Mechanics*. Charles University.
- LAGERSTROM, P. A., COLE, J. D. & TRILLING, L. 1949 *Problems in the Theory of Viscous Compressible Fluids (Monograph)*. California Institute of Technology.
- LASSEUX, D. & VALDES PARADA, F. J. 2017 On the development of Darcy’s law to include inertial and slip effects. *C. R. Méc.* **345**, 660–669.
- LASSEUX, D., VALDES PARADA, F. J., OCHOA TAPIA, J. A. & GOYEAU, B. 2014 A macroscopic model for slightly compressible gas slip-flow in homogeneous porous media. *Phys. Fluids* **26**, 053102.
- LASSEUX, D., VALDES PARADA, F. J. & PORTER, M. L. 2016 An improved macroscopic model for gas slip flow in porous media. *J. Fluid Mech.* **805**, 118–146.
- LEAL, L. G. 2010 *Advanced Transport Phenomena*. Cambridge University Press.

- LIONS, J. L. & MASMOUDI, N. 1998 Incompressible limit for a viscous compressible limit. *J. Math. Pures Appl.* **77** (6), 585–627.
- LUGO-MENDEZ, H. D., VALDES-PARADA, F. J., PORTER, M. L., WOOD, B. D. & OCHOA-TAPIA, J. A. 2015 Upscaling diffusion and nonlinear reactive mass transport in homogeneous porous media. *Trans. Porous Med.* **107** (3), 683–716.
- MASMOUDI, N. 2000 Asymptotic problems and compressible and incompressible limits. In *Advances in Mathematical Fluid Mechanics* (ed. J. Málek, J. Nečas & M. Rokyta), pp. 119–158. Springer.
- MASMOUDI, N. 2002 Homogenization of the compressible Navier–Stokes equations in a porous medium. *ESAIM: Control Optim. Calculus Variations* **8**, 885–906.
- MASMOUDI, N. 2007 Examples of singular limits in hydrodynamics. In *Handbook of Differential Equations: Evolutionary Equations* (ed. C. M. Dafermos & E. Feireisl), vol. 3, pp. 195–275. Elsevier.
- MORSE, P. M. & INGARD, K. U. 1968 *Theoretical Acoustics*. McGraw-Hill.
- MUNZ, C. D., DUMBSER, M. & ROLLE, S. 2007 Linearized acoustic perturbation equations for low Mach number flow with variable density and temperature. *J. Comput. Phys.* **224**, 352–364.
- MUNZ, C. D., ROLLER, S., KLEIN, R. & GERATZ, K. J. 2003 The extension of incompressible flow solvers to the weakly compressible regime. *Comput. Fluids* **32**, 173–196.
- MUSKAT, M. 1937 *The Flow of Homogeneous Fluids Through Porous Media*. McGraw-Hill.
- MUSKAT, M. 1949 *Physical Principles of Oil Production*. McGraw-Hill.
- PANTON, R. L. 2013 *Incompressible Flow*, 4th edn. Wiley.
- PIERCE, A. D. 1981 *Acoustics: An Introduction to Its Physical Principles and Applications*. McGraw-Hill.
- RAYLEIGH, LORD (J. W. STRUTT) 1945 *The Theory of Sound*, vol. 2. Dover.
- SANTOS-SANCHEZ, R., VALDES-PARADA, F. J. & CHIRINO, Y. I. 2016 Upscaling diffusion and reaction processes in multicellular systems considering different cell populations. *Chem. Engng Sci.* **142** (13), 144–164.
- SCHEIDEGGER, A. E. 1974 *The Physics of Flow through Porous Media*. University of Toronto Press.
- SCHOCHET, S. 1987a Hyperbolic–hyperbolic singular limits. *Commun. Part. Diff. Equ.* **12** (6), 589–632.
- SCHOCHET, S. 1987b Singular limits in bounded domains for quasilinear symmetric hyperbolic systems having a vorticity equation. *J. Differ. Equ.* **68** (3), 400–428.
- SCHOCHET, S. 2005 The mathematical theory of low Mach number flows. *Math. Modeling Numer. Anal.* **39** (3), 441–458.
- TEMKIN, S. 1981 *Elements of Acoustics*. Wiley.
- VALDES-PARADA, F. J. & AGUILAR-MADERA, C. G. 2011 Upscaling mass transport with homogeneous and heterogeneous reaction in porous media. *Chem. Engng* **24**, 1453–1458.
- VALDES-PARADA, F. J., AGUILAR-MADERA, C. G. & ALVAREZ-RAMIREZ, J. 2011 On diffusion, dispersion and reaction in porous media. *Chem. Engng Sci.* **66** (10), 2177–2190.
- VALDES-PARADA, F. J., LASSEUX, D. & WHITAKER, S. 2017 Diffusion and heterogeneous reaction in porous media: the macroscale model revisited. *Intl J. Chem. Reactor Engng* **15** (6), 24–30.
- VALDES-PARADA, F. J., PORTER, M. L., NARAYANASWAMY, K., FORD, R. M. & WOOD, B. D. 2009 Upscaling microbial chemotaxis in porous media. *Adv. Water Resour.* **32** (9), 1413–1428.
- WESSELING, P. 2001 *Principles of Computational Fluid Dynamics*. Springer.
- WHITAKER, S. 1966 The equations of motion in porous media. *Chem. Engng Sci.* **21** (3), 291–300.
- WHITAKER, S. 1986 Flow in porous media. Part I. A theoretical derivation of Darcy’s law. *Trans. Porous Med.* **1**, 3–25.
- WHITAKER, S. 1999 *The Method of Volume Averaging*. Kluwer Academic.
- WOOD, B. D. & WHITAKER, S. 1997 Diffusion and reaction in biofilms. *Chem. Engng Sci.* **53** (3), 397–425.
- WOOD, B. D. & WHITAKER, S. 1999 Multi-species diffusion and reaction in biofilms and cellular media. *Chem. Engng Sci.* **55** (17), 3397–3418.
- WU, T. Y. 1956 Small perturbations in the unsteady flow of a compressible, viscous and heat conducting fluid. *J. Math. Phys.* **35**, 13–27.